Publication 5

Ge Y., Heczko O., Söderberg O. and Lindroos V. K. Various magnetic domain structures in a Ni-Mn-Ga martensite exhibiting magnetic shape memory effect. Journal of Applied Physics, **96**, (2004), 2159-2163.

© 2004 American Institute of Physics

Reprinted with permission from American Institute of Physics.

Various magnetic domain structures in a Ni–Mn–Ga martensite exhibiting magnetic shape memory effect

Y. Ge, O. Heczko, O. Söderberg, and V. K. Lindroos
Laboratory of Physical Metallurgy and Materials Science, Helsinki University of Technology, P.O. Box 6200, Fi-02015 HUT, Finland

(Received 25 February 2004; accepted 25 May 2004)

Magnetic domain structures of the Ni–Mn–Ga martensite were observed by means of type I and type II magnetic contrast in scanning electron microscope. The different configuration of magnetic domain patterns coupled together with the twin structures were studied in multivariant, two-variant, and single-variant martensite. The martensitic band contains broad stripelike magnetic domains following the easy axis of magnetization, i.e., the crystallographic *c* axis. These stripe domains are connected by 90° domain walls creating a staircaselike structure in the adjoining bands. It is found that the internal twins, substructures of the martensite twin domains, are distorted into a zig–zag shape in order to accommodate the main band magnetization. Furthermore, the dagger-shaped stripe domains occur only when the internal twins are present. When the sample exhibits the single-variant state, the internal twins disappear totally and the stripe magnetic domains spread over the whole specimen. The configuration observed here for the magnetic microstructure together with the crystallographic microstructure can help in understanding the magnetic shape memory effect. © *2004 American Institute of Physics*. [DOI: 10.1063/1.1773381]

I. INTRODUCTION

The Ni–Mn–Ga alloys have been studied for years. In a martensitic phase transformation some of Ni–Mn–Ga alloys transform to a five-layered modulated tetragonal structure (5M), which can show a large magnetic-field-induced strain (MFIS) of 0.2%–6%.[1–5] This shape change referred to as the magnetic shape memory effect (MSME) is due to the rearrangement of martensitic twin variants in the magnetic field.

The crystal structure in Ni–Mn–Ga alloys is strongly composition dependent. Even though the parent phase exhibits the cubic Heusler-type structure, the martensite structures can be nonmodulated tetragonal (T), seven-layered modulated, approximately orthorhombic structure (7M) or five-layered modulated, approximately tetragonal structure. Furthermore, occasionally also a mixture of different martensite types may exist.[5] In such alloys as studied in the present work with the 5M martensite structure, the easy axis of magnetization in martensite always coincides with the shortest crystallographic axis.[3–8] During cooling from the cubic parent phase to the martensitic structure, the twins are accommodating the strain occurring in transformation. These twins also can have a substructure of internal twins, which has been confirmed by x-ray diffraction.[9] After the transformation the layered tetragonal crystal contains three twin variants with different orientation of the easy magnetization axis (*c*-axis in the cubic coordinates) separated by twin boundary. Of these variants the one having the easy magnetization axis along the applied magnetic field starts to grow at the expense of the other variants. This leads to the martensitic twin boundary motion which is the basis of the mechanics of MSME.[1,3]

Therefore, the interaction of magnetic domains and the twinned martensitic crystal structure play an important role during the rearrangement of the twin variants. This interaction has been studied by several techniques: Bitter and scanning electron microscope (SEM) methods,[10] with magneto-optical method,[11] magnetic force microscopy (MFM),[12] interference-contrast-colloid (ICC),[13] and Lorentz transmission electron microscopy (TEM).[14] The results show that the magnetic domain structure changes during the phase transformation and during the magnetization process. Furthermore, it has been confirmed that the magnetic domains are coupled with martensitic twins. However, so far no results have been reported on the interaction of the magnetic domain structure and the internal twins.

The type I and type II magnetic contrasts of SEM (Ref. 15) are employed in the present work to investigate magnetic domain structure together with the twin structure of 5M martensite. The type I contrast is obtained from the interaction of secondary electrons with the stray magnetic field above the specimen surface and, consequently, it is available only through the secondary electron image (SEI). An overview of underlying magnetic domain structure without particular details is revealed with this technique. The type II contrast observed by the backscattered electron image (BEI), is connected with both the absorbed magnetic contrast and the deflected magnetic contrast, which can be detected with different geometry configuration of specimen, electron beam, and detector.[16] The type II contrast reveals detailed domain patterns of the surface. In the present work these techniques are applied to study the detailed magnetic structures in connection with the multivariant, two-variant, and single-variant structures of the Ni–Mn–Ga 5M martensite.

II. EXPERIMENTAL PROCEDURES

The ingot of the polycrystalline $Ni_{48.9}Mn_{30.8}Ga_{20.3}$ alloy was manufactured using a modified Bridgman method at Outokumpu Research Oy, Finland. After casting, it was at

 © 2004 American Institute of Physics

first homogenized in a vacuum quartz ampoule for 48 h at 1273 K, then directly annealed for 72 h at 1073 K, and finally cooled in air to room temperature. The phase transformation and magnetic transition temperatures of the annealed alloy were determined with a differential scanning calorimeter (DSC) of type Linkam-600 and the ac low-field magnetic susceptibility method. The Curie point of the alloy was $T_c = 370$ K, while the start and finish transformation temperatures were $M_s = 324$ K and $M_f = 321$ K for the martensitic reaction as well as $A_s = 332$ K and $A_f = 335$ K for the reverse reaction.

The single-crystal specimens for the SEM studies were spark-cut to the dimensions of 3 mm × 4 mm × 6 mm from a large grain of the polycrystalline ingot. The specimens were wet-ground and electropolished in a solution of 25% nitric acid using 12 V and 0.1 A/mm^2 at 273 K.

The orientation and crystal structure of the specimens were studied with a Philips X'pert x-ray diffractometer. It was confirmed that the edges of the specimens were nearly parallel to the ⟨100⟩ directions (in the cubic coordinates) with a maximum deviation of 6°. Furthermore, it was shown that the material has the modulated five-layered, close to tetragonal martensitic structure at ambient temperature.[17] Specimens prepared in this manner exhibited the magnetic-field-induced strain of approximately 6% in the MSM measurement. The details of the method are given elsewhere.[6]

In order to study the different variant states of the 5M structure, the specimen was at first studied in a multivariant state, then transformed to a two-state and after the investigation of this structure, the specimen was finally brought to the single-variant state. The multivariant martensitic state occurred in the specimen as-prepared, due to the twin variant accommodation in the martensitic transformation. The two-variant state was obtained by successive compressions followed by the controlled magnetization. In the third stage, the single-variant state resulted from magnetizing the sample to saturation.

The magnetic contrast observations and composition analysis were carried out on SEM LEO-1450 equipped with energy dispersive spectroscopy (EDS). Both type I and II magnetic contrast were used to investigate the detailed magnetic structure. In these studies the surface of specimen was normal to the electron beam. The scintillator type secondary electron detector was placed in a side position and the collector bias voltage was set at +300 V. The four-quadrant solid state diode backscattered detector was situated just below the objective lens. The composition contrast (COMPO) mode of BEI was obtained by using the sum signal from all four quadrants. The topography contrast (TOPO) mode of BEI was obtained by turning off two diagonal quadrants and using the difference signal from the two other diagonal quadrants. In order to achieve optimum contrast in the magnetic contrast modes, the accelerating voltage in SEI was 5 kV and in BEI 30 kV. To avoid local overheating of the specimen, the probe current was adjusted to the lowest value that still could give the maximum contrast.

III. RESULTS AND DISCUSSIONS

After the martensitic reaction, the structure exhibits the multivariant twinning system in order to accommodate the transformation strain occurring during the transformation from the cubic to the tetragonal phase. Figure 1(a) shows the magnetic domain structure together with martensitic twin variant structure of the specimen in the multivariant state. The viewed area was selected in such a way that it shows only those martensitic twin bands having the *c*-axis in plane of the surface. They are relatively narrow with the width in the region of 100–200 μm. Figure 1(a) shows also that the major twin bands consist of some fine internal substructures. These parallel thin lines are regarded as belonging to the internal twinning. In Fig. 1(a), the SEI shows magnetic domain structure where the magnetization direction was parallel to the secondary detector. When the specimen was rotated 90°, the domain structure of alternative bands appears, as shown in Fig. 1(c). Since the type I contrast arises from the outside magnetic stray field of the specimen, it has limited resolution. The domain structures shown in Figs. 1(a) and 1(c) are more or less like stripe patterns following the easy magnetization axis in each martensitic band. However, even the type II contrast is poor in the multivariant state and the approximately stripe pattern is clearly established in Fig. 1(b) revealing more details. BEI showed the internal twins more clearly and in magnification in Fig. 1(d), it can be seen in both the magnetic domain structure and the internal twins near the twin boundary. In the upper twin band the magnetic domains form an approximately stripe pattern with some dagger-shaped domains. The lower twin band appears as more like the stripe pattern of magnetic domains. They are clearly visible due to the bending of the internal twins. Such a bending will be discussed in the following section. Furthermore, it is worthwhile to note that the particular magnetic domain structure is limited inside the twin band.

The dagger-shaped domains observed in Fig. 1(d) are the closure domains compensating the magnetic charge occurring on the twin boundary. This is similar to the observed pattern across the grain boundary.[18] In an ideal homogenous case of two adjoining twin variants having the symmetrical arrangement of the magnetization which follows the easy axes, there is no magnetic charge. However, when the sample is in the multivariant state the internal twin structure can disturb this symmetrical arrangement. The resulting slight deviations can induce the magnetic charges and lead to the appearance of the closure domains. The existence of the complex internal structure can be also inferred from the secondary electron images, mapping the magnetic stray field above the specimen. This is confirmed with the fact that the dagger-shaped domains disappear when the sample is in the more homogenous two-variant state.

Using a repeated compression and controlled magnetization process the specimen was transformed from the multivariant state to the two-variant state. Now, there were only two alternating twin bands in the specimen with *c*-axis in the plane of surface. Both the magnetic domain contrast and the domain wall contrast are greatly enhanced and they are clearly observed by BEI in Fig. 2. The stripe domain pattern

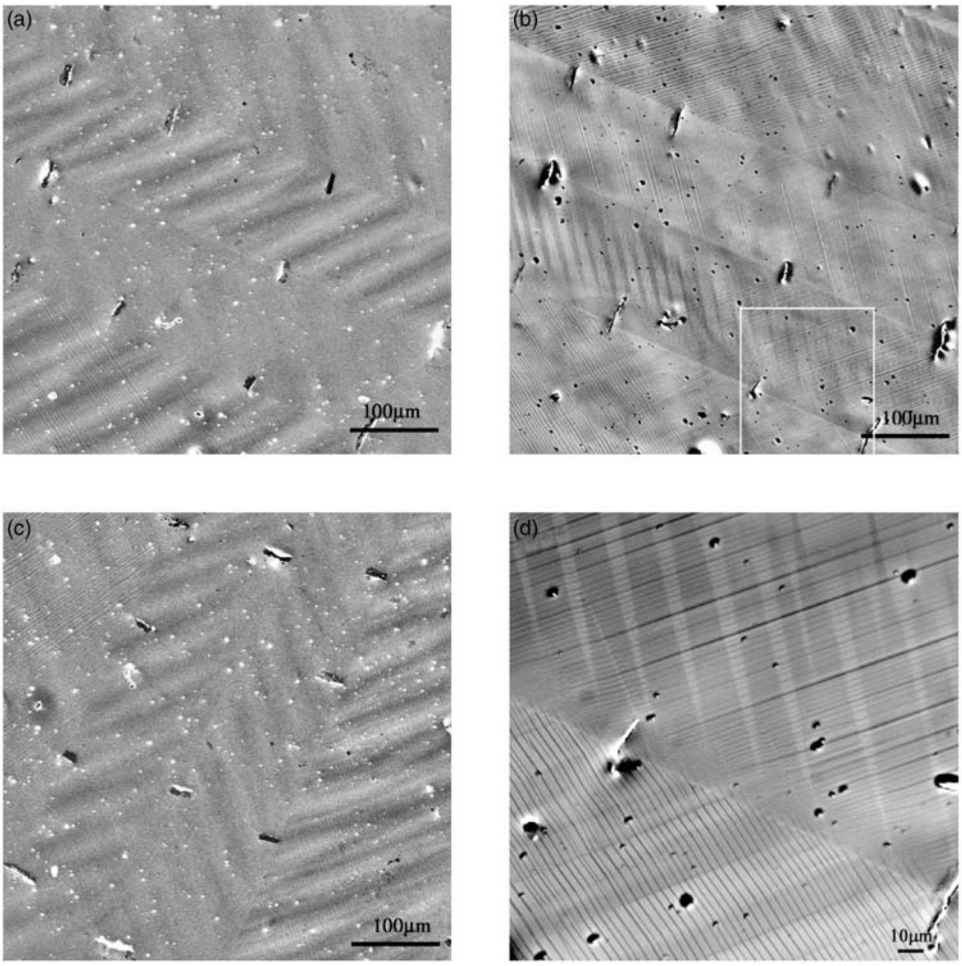

FIG. 1. Image of the multivariant specimen (a) by SEI and (b) by BEI; (c) The same area after 90° rotation by SEI; (d) The magnified image from the rectangular area in (b) by BEI.

occupies the whole area and no internal twins are visible. Figure 2 shows the stripe domains magnetized parallel and antiparallel to the easy [001] direction. The observed structure is in agreement with the previous results with Bitter technique[10] and the ones obtained with the magneto-optic film.[11]

The stripe domains in the adjoining bands follow the easy magnetization axis and thus create a staircaselike structure. The domains are connected by 90° domain walls, which coincide with the twin boundary. The high contrast between parallel and antiparallel domains decreases the visibility of the 180° domain wall contrast. On the other hand, the 90° domain wall has a very high contrast, indicated by alternative white and dark twin boundaries. The overall arrangement of the twin bands and the magnetic domains in two variant specimen is discussed in more detail in Ref. 10. A rough estimation of the average domain width calculated from the basic magnetic parameters and the size of the specimen is in the region of 10–20 μm, which agrees with the width measured from the images. According to the domain contrast the magnetization direction could be easily determined,[19] which is indicated by the arrows in Fig. 2.

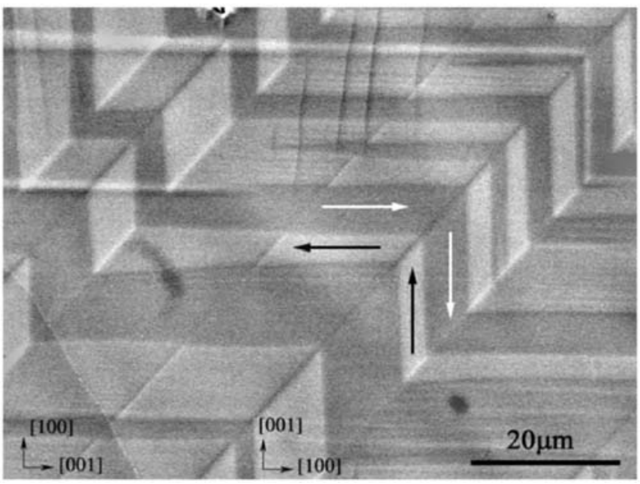

FIG. 2. The two-variant specimen with the magnetic stripe domain pattern coupled with the twin band (BEI).

According to the mechanism of the type II contrast, it is possible to separate the magnetic domain contrast and the magnetic domain wall contrast with an annular symmetry backscattered detector.[16] Figures 3(a) and 3(b) are the type II images made in COMPO mode and TOPO mode, respectively. With COMPO mode we obtained a good domain wall contrast and a domain contrast between the 180° domains. The domain wall contrast totally disappears in TOPO mode. Instead, the contrast between the 90° domains is more apparent. Consequently, these two methods can complement each other and give all information needed about the domain structure.

In the two-variant specimen, the substructure, the inter-

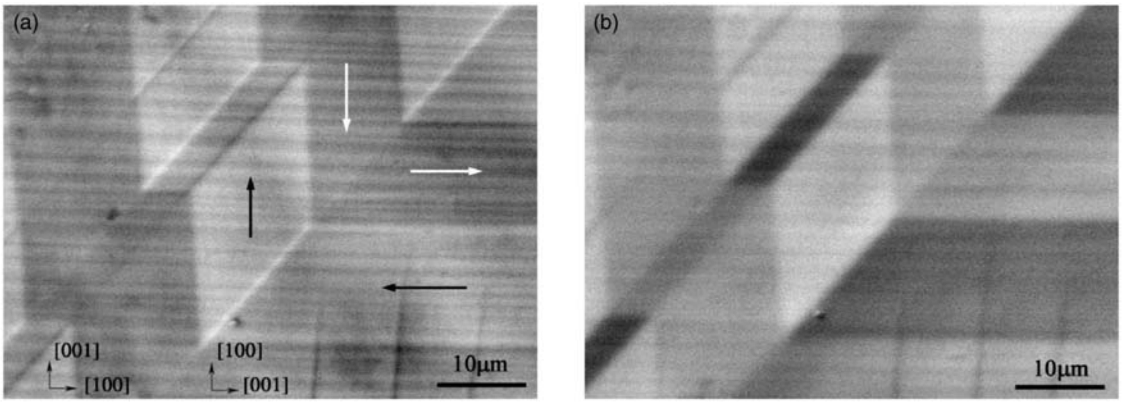

FIG. 3. The type II magnetic contrast of the two-variant specimen; (a) in COMPO mode (b) in TOPO mode.

nal twins, disappeared in the majority of the twin bands. However, the residual internal twins remain still in some areas. An example of two adjoining twin variants with internal twins is shown in Fig. 4. Both variants contain a stripe magnetic domain structure, however in the left twin band the domain structure is more dagger-shaped. The stripe magnetic domains meet at twin boundary and fit each other very well similarly as shown in Fig. 2. However in this case (Fig. 4), the twin boundary is somehow spread out and no good contrast, either magnetic or crystallographic, can be obtained. The wide twin boundary could be caused by a complex intersecting of the internal twins. Both variants contain the internal twins observed as light and dark thin lines inside the main twin bands. The internal twins are nearly perpendicular to the magnetization direction and have a peculiar zig–zag pattern following the magnetic domains. This suggests that there is a strong interaction between magnetic domains and internal twins.

The origin of the zig–zag pattern can be explained as follows. A single internal twin has its easy magnetization direction along its trace in the observing plane, which is perpendicular to the main magnetization direction indicated by the stripe magnetic domains. Due to interaction with the magnetic field of the main magnetic domain, the magnetization of the internal twin will rotate away from its own easy axis towards the main magnetization direction. This will increase the magnetic energy stored to the internal twin. As the twinned martensitic structure is very flexible, the magnetic energy can be reduced by deforming the internal twin. The critical stress to deform the martensite is given by twinning stress, σ_{tw}. When the magnetic energy stored in the internal twin exceeds the elastic energy, $\sigma_{tw}\varepsilon_0$, where ε_0 is the tetragonal distortion, the reorientation of the lattice occurs.[20] The local reorientation, i.e., the rotation of the crystallographic *c*-axis locally to the direction of the main magnetization, results in apparent tilting of the internal twins. In more quantitative terms, the twinning stress for this material is in the range of 1–5 MPa (Refs. 20 and 21) and the tetragonal distortion $\varepsilon_0=6\%$, which gives the elastic energy needed for the lattice reorientation in the range of $0.6-3\times10^5$ J/m^3. The maximum magnetic energy stored is given by the anisotropy energy $K_u=1.6\times10^5$ J/m^3.[8] From the energy comparison it is apparent that the reorientation can occur to some degree depending on the magnitude of the twinning stress. The tilting of the internal twins occurs in the opposite directions in the magnetic domains with parallel and antiparallel magnetization resulting in the observed zig–zag pattern. Close observation of the zig–zag pattern of internal twins suggests that the lattice is not homogeneously malleable as the zig–zag lines are not parallel and create a slightly irregular pattern. This agrees with the stress–strain measurements which indicate a wide distribution of the magnitude of the twinning stress.[21]

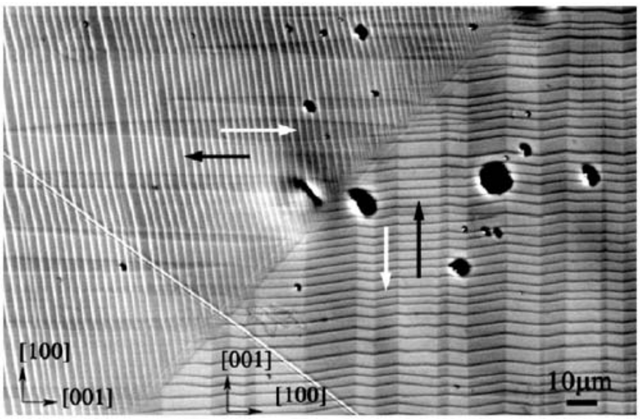

FIG. 4. The area in which the twin boundary and the internal twins are present in the two-variant specimen (BEI).

It is found that the dagger-shaped stripe domain pattern is only observed in the twin band if the internal twins are present. However, the perfect stripe domain pattern can also be observed in the internal twin area. This indicates that the specific crystal orientation of the internal twins determine the magnetic microstructure by affecting the charge imbalance or breaking the symmetry of the magnetization arrangements in adjoining twin bands. On this basis it can be suggested that the twinned structure without the internal twinning and with the perfect stripe magnetic domain pattern is more favorable for the twin boundary motion during the magnetization process and, consequently, for the existence of MSME.

In the fully magnetized specimen, no twin band is visible except some residual twin bands near the edge of the specimen. The specimen can be considered to be in a single-variant state. Also, the internal twins have disappeared to-

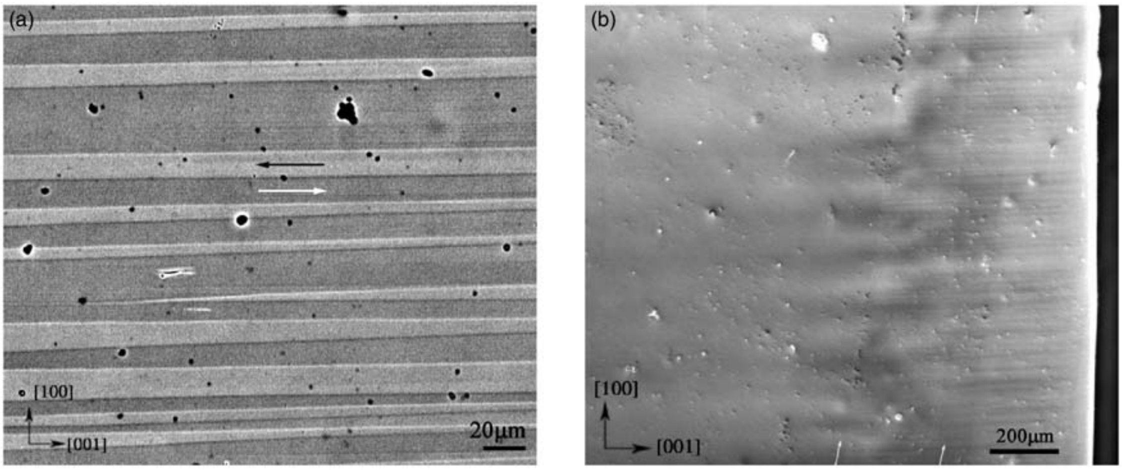

FIG. 5. The single-variant sample with stripe domain is imaged by (a) type II contrast, and (b) type I contrast. [In (b) the twin boundary of the residual variant is marked by the arrows.]

tally. The stripe magnetic domains run along the magnetization direction through the whole specimen, as shown in Fig. 5(a). The domain width varies in the range of 1–30 μm. The type I contrast shows the stripe domain branching into fine stripes at the edge of specimen [Fig. 5(b)], where the residual twins with the easy magnetization direction perpendicular to the surface plane with labyrinth domain structure exist.

IV. CONCLUSIONS

The crystallographic and the magnetic microstructures were studied in three martensitic states of a Ni–Mn–Ga alloy with 5M structure. Based on the present study the following conclusions can be drawn:

(1) In the multivariant state the martensitic twins contain the internal twins and the magnetic domain pattern in the main twin bands consists mostly of the stripe domains.
(2) In the two-variant state, most of the internal twins have disappeared, and the stripe magnetic domains are running through twin bands. The twin boundary coincides with the 90° magnetic domain wall. If the internal twins remain in the martensitic variant then the dagger-shaped domains occur. They compensate for the magnetic charge imbalance in adjoining twins. It seems that the dagger-shaped or the stripe domain patterns are determined by the specific orientation of the internal twins. The internal twins are bent into a zig–zag shape due to the interaction with the magnetization in the stripe domains.
(3) In the sample with the single-variant state, long stripe domains run through the whole specimen. Consequently, the stripe magnetic domain pattern may facilitate the twin boundary motion.

ACKNOWLEDGMENTS

The funding support of the National Technology Agency (Tekes), Finland, and the consortium of Finnish companies (Outokumpu Research Centre, Metso Oyj, Nokia Research Center and AdaptaMat Ltd.) as well as The Academy of Finland for this work is gratefully acknowledged. The authors would like to thank Dr. Erkki Heikinheimo for his good advice.

[1] K. Ullakko, J. K. Huang, C. Kantner, R. C. O'Handley, and V. V. Kokorin, Appl. Phys. Lett. **69**, 1966 (1996).
[2] R. D. James, R. Tickle, and M. Wuttig, Mater. Sci. Eng., A **273–275**, 320 (1999).
[3] O. Heczko, A. Sozinov, and K. Ullakko, IEEE Trans. Magn. **36**, 3266 (2000).
[4] S. J. Murray, M. Marioni, S. M. Allen, R. C. O'Handley, and T. A. Lograsso, Appl. Phys. Lett. **77**, 886 (2000).
[5] A. Sozinov, A. A. Likhachev, N. Lanska, O. Söderberg, K. Ullakko, and V. K. Lindroos, Proc. SPIE **5053**, 586 (2003).
[6] O. Heczko, L. Straka, and K. Ullakko, J. Phys. IV **112**, 959 (2003).
[7] A. Sozinov, A. A. Likhachev, and K. Ullakko, IEEE Trans. Magn. **38**, 2814 (2002).
[8] L. Straka and O. Heczko, J. Appl. Phys. **93**, 8636 (2003).
[9] G. Mogylnyy, I. Glavatskyy, N. Glavatska, O. Soderberg, Y. Ge, and V. K. Lindroos, Scr. Mater. **48**, 1427 (2003)
[10] O. Heczko, K. Jurek, and K. Ullakko, J. Magn. Magn. Mater. **226–230**, 996 (2001).
[11] A. Sozinov, Y. Ezer, G. Kimmel, P. Yakovenko, D. Giller, Y. Wolfus, Y. Yesherun, K. Ullakko, and V. K. Lindroos, J. Phys. IV **11**, Pr8–311 (2001).
[12] Qi Pan and R. D. James, J. Appl. Phys. **87**, 4702 (2000).
[13] H. D. Chopra, C. Ji, and V. V. Kokorin, Phys. Rev. B **61**, 14913 (2000).
[14] M. De Graef, M. A. Willard, M. E. McHenry, and Y. Zhu, IEEE Trans. Magn. **37**, 2663 (2001)
[15] L. Reimer, *Scanning Electron Microscopy* (Springer, New York, 1998), p. 290.
[16] L. Pogany, K. Ramstock, and A. Hubert, Scanning **14**, 263 (1992).
[17] Y. Ge, A. Sozinov, O. Söderberg, N. Lanska, K. Ullakko, and V. K. Lindroos, J. Phys. IV **112**, 921 (2003).
[18] A. Hubert and R. Schafer, *Magnetic Domains: The Analysis of Magnetic Microstructures* (Springer, New York, 1998), p. 415.
[19] D. C. Joy, H. J. Leamy, and S. D. Ferris, Appl. Phys. Lett. **28**, 466 (1976).
[20] O. Heczko and L. Straka, J. Appl. Phys. **94**, 7139 (2003).
[21] K. Koho, J. Vimpari, L. Straka, N. Lanska, O. Söderberg, O. Heczko, K. Ullakko, and V. K. Lindroos, J. Phys. IV **112**, 943 (2003).